

Woollam, J., Münchmeyer, J., Tilmann, F.,
Rietbrock, A., Lange, D., Bornstein, T., Diehl, T.,
Giunchi, C., Haslinger, F., Jozinović, D., Michelini, A.,
Saul, J., Soto, H. (2022): SeisBench—A Toolbox for
Machine Learning in Seismology. - Seismological
Research Letters, 93, 3, 1695-1709.

<https://doi.org/10.1785/0220210324>

SeisBench - A Toolbox for Machine Learning in Seismology

Jack Woollam^{1, *, #}, Jannes Münchmeyer^{2, 3, #}, Frederik Tilmann^{2, 7}, Andreas Rietbrock¹, Dietrich Lange⁶, Thomas Bornstein², Tobias Diehl⁴, Carlo Giunchi⁵, Florian Haslinger⁴, Dario Jozinović^{8, 9}, Alberto Michelini⁸, Joachim Saul², and Hugo Soto²

¹Geophysical Institute (GPI), Karlsruhe Institute of Technology, Karlsruhe, Germany

²Deutsches GeoForschungsZentrum GFZ, Potsdam, Germany

³Institut für Informatik, Humboldt-Universität zu Berlin, Berlin, Germany

⁴Swiss Seismological Service, ETH Zurich, Zurich, Switzerland

⁵Istituto Nazionale di Geofisica e Vulcanologia, Sezione di Pisa, Pisa, Italy

⁶GEOMAR Helmholtz Centre for Ocean Research Kiel, Kiel, Germany

⁷Institut für geologische Wissenschaften, Freie Universität Berlin, Berlin, Germany

⁸Istituto Nazionale di Geofisica e Vulcanologia, Roma, Italy

⁹Università degli Studi Roma Tre, Largo San Leonardo Murialdo 1, Rome, Italy

*corresponding author

#equal contribution

Abstract

Machine Learning (ML) methods have seen widespread adoption in seismology in recent years. The ability of these techniques to efficiently infer the statistical properties of large datasets often provides significant improvements over traditional techniques when the number of data are large (millions of examples). With the entire spectrum of seismological tasks, e.g., seismic picking and detection, magnitude and source property estimation, ground motion prediction, hypocentre determination; among others, now incorporating ML approaches, numerous models are emerging as these techniques are further adopted within seismology. To evaluate these algorithms, quality controlled benchmark datasets that contain representative class distributions are vital. In addition to this, models require implementation through a common framework to facilitate comparison. Accessing these various benchmark datasets for training and implementing the standardization of models is currently a time-consuming process, hindering further advancement of ML techniques within seismology. These development bottlenecks also affect 'practitioners' seeking to deploy the latest models on seismic data, without having to necessarily learn entirely new ML frameworks to perform this task. We present SeisBench as a software package to tackle these issues. SeisBench is an open-source framework for deploying ML in seismology - available via GitHub. SeisBench standardises access to both models and datasets, whilst also providing a range of common processing and data augmentation operations through the API. Through SeisBench, users can access several seismological ML models and benchmark datasets available in the literature via a single interface. SeisBench is built to be extensible, with community involvement encouraged to expand the package. Having such frameworks available for accessing leading ML models forms an essential tool for seismologists seeking to iterate and apply the next generation of ML techniques to seismic data.

23 Introduction

24 Seismology has always been a ‘data-rich’ field. With the continued advances in computational power,
25 along with the increased use of high-density density deployments of nodal geophones, the seismic wavefield
26 is now recorded with increasing resolution and fidelity. Such advances are not just exclusive to seismology;
27 within science in general, larger, more detailed datasets are being compiled. Machine Learning (ML) has
28 risen to prominence as a set of techniques to best exploit the information contained in such extensive
29 datasets. Often termed ‘data-driven’ methods, ML tools probabilistically model the statistical properties
30 of a given dataset to perform inference for a given task. As datasets get larger, and the inference step
31 becomes a more tractable problem, these techniques are now achieving state-of-the-art performance across
32 the entire spectrum of scientific fields. In many areas performance is outpacing the human analyst.

33 Although some pioneering works harnessed neural networks for seismological applications (e.g Wang
34 and Teng, 1997; Valentine and Trampert, 2012), for many years such techniques did not find wider
35 usage in seismology until approximately three years ago. The possibility to assemble large datasets,
36 massive parallelisation on commodity hardware through GPU computing, algorithmic improvements and,
37 importantly, the availability of software frameworks such as PyTorch (Paszke et al., 2017) and Tensorflow
38 (Abadi et al., 2016) has driven a wave of applications of ML techniques to classical seismological problems,
39 including earthquake phase identification (Zhu and Beroza, 2019; Ross, Meier, Hauksson and Heaton,
40 2018; Woollam et al., 2019; Zhou et al., 2019; Wang et al., 2019), earthquake detection (Mousavi, Zhu,
41 Sheng and Beroza, 2019; Mousavi et al., 2020; Zhou et al., 2019; Perol et al., 2018; Dokht et al., 2019;
42 Pardo et al., 2019), magnitude estimation (Lomax et al., 2019; Mousavi and Beroza, 2020; van den Ende
43 and Ampuero, 2020; Münchmeyer et al., 2021*a*), and earthquake early warning (Kong et al., 2016; Li
44 et al., 2018; Münchmeyer et al., 2021*b*), amongst others.

45 From these initial works, a natural question arises: which ML techniques perform best for each
46 task? Answering this question is not trivial, as each study uses different data, different ML frameworks
47 for algorithm development, and different assessment metrics. Benchmarking and comparison studies
48 are, therefore, inherently difficult. The varying data used during training is a particular problem, as the
49 variable nature of earthquake source, propagation medium and site conditions mean that the performance
50 of a model trained on one region or environment might not be directly compared to a model trained in a
51 different region. To enable fair comparisons of models and model architectures over a range of possible
52 environments, benchmark datasets are essential.

53 Labelled benchmark datasets have been vital to rapid-progress in various classic ML application
54 domains, most prominently computer-vision (MNIST, Deng, 2012; ImageNet Deng et al., 2009), and
55 natural language processing (Sentiment140, Go et al., 2009), as they allow for easy assessment of which
56 ML algorithms perform best. Creating such quality-controlled datasets takes, however, a significant
57 amount of time. Benchmark datasets perform this step for users ensuring comparability of different

58 studies, greatly accelerating the development and testing of novel ML algorithms. With ML methods
59 only recently being widely adopted in seismology, historically, there were no benchmark datasets available
60 for comparison works. This situation is now changing with the value of such datasets widely recognised.
61 The seismological benchmark datasets now emerging (e.g. LenDB, Magrini et al., 2020; INSTANCE,
62 Michelini et al., 2021; NEIC, Yeck et al., 2021; STEAD, Mousavi, Sheng, Zhu and Beroza, 2019) already
63 cover a wide-range of potential seismic environments (e.g. global, regional, local), essential factors for
64 training robust algorithms.

65 However, the availability of new benchmark datasets does not completely solve the comparison prob-
66 lem. Remaining issues include the differing data formats employed by different benchmarks, and the
67 specific framework libraries ML researchers use to implement their models e.g. PyTorch, Tensorflow,
68 Keras (Chollet et al., 2015), Sklearn (Pedregosa et al., 2011), add complexity to any comparison work.
69 Any benchmarking must, therefore, check that operations applied within each library are directly com-
70 parable, with no discrepancies in implementation.

71 The easy availability of both benchmark datasets, and standardised access to the latest models, are
72 crucial ingredients for advancing the state-of-the-art. As this problem is common to any application
73 based on ML (Király et al., 2021), tools have been developed in other fields to provide researchers
74 with easy access to models and benchmark datasets (e.g. FLAIR, Akbik et al., 2019, natural language
75 processing toolbox). These continue to be widely used, evidence of their ability to aid development.

76 To date, we are unaware of the availability of such software in seismology. The outlined bottlenecks
77 affect a wide range of potential users of ML. For the 'practitioner', who wishes to apply ML models to their
78 seismic data, they are currently facing significant hurdles, as they would have to learn specific frameworks
79 to integrate the latest ML algorithms into their workflows. For the 'expert' interested in developing novel
80 techniques, they currently have to integrate various models, testing over varying datasets', which may
81 be in differing formats. Without any frameworks or toolboxes to help with these problems, researchers
82 must construct such comparison pipelines from scratch. This is a significant undertaking. These factors
83 are currently hindering more widespread ML adoption in seismology and are limiting progress in the
84 development of the next generation of ML methods. Tackling these problems is key if the seismological
85 community is to accelerate the development of ML techniques for seismic tasks and promote further
86 adoption of ML within the field. We have built the SeisBench open-source software package to address
87 these issues.

88 The SeisBench ML framework

89 SeisBench provides a unified point-of-access for ML development and application within the seismological
90 community. Built in Python ¹, it integrates both state-of-the-art models and datasets in a single frame-
91 work. Figure 1 visually highlights this concept, introducing the core components of SeisBench. The
92 range of datasets presented in the initial release include currently published seismological benchmark
93 datasets from the literature, directly integrated into the package.

94 SeisBench also provides access to additional custom benchmark datasets which are made newly avail-
95 able in the initial release of the software. As all datasets within SeisBench adhere to a common format,
96 users can compare their algorithms across a range of seismic environments, from detecting global signals
97 to local settings. Models are accessed through a unified interface – enabling easy comparison of differing
98 approaches. Whilst the model interface is designed towards integrating various deep learning models, the
99 types of models that can be built and compared in SeisBench are not just limited to deep learning-based
100 routines; traditional methods can also be directly deployed and integrated into comparison workflows.
101 Finally, typical data augmentation and pre-processing steps are provided through an augmentation API.
102 With seismologists, and general ML practitioners often, re-implementing the same operations for data
103 pre-processing and augmentation, inclusion of many of the standard processes and augmentations in
104 SeisBench will further facilitate faster model development.

105 SeisBench is designed to be generally applicable to the entire spectrum of general seismological tasks,
106 such as source parameter estimation, magnitude estimation, ground motion prediction. Whilst the
107 currently included models relate specifically to picking and event detection, SeisBench is suitable for
108 many other seismological tasks based on waveform analysis. The extensible nature of the API means
109 that any parameter from a datasets’ metadata can be used as a label (target variable), enabling the
110 construction of any supervised classification pipeline.

111 Data - Standardising access to Benchmark datasets

112 A standardised format for seismic waveforms and metadata information

113 The SeisBench *data* module contains functionality to read and process seismological datasets which have
114 been converted into the SeisBench standardised format. Using a standardised framework enables the
115 construction or conversion of varying benchmark seismological datasets. The dataset format follows
116 a typical approach encountered within the ML community (Figure 2), where the waveforms (training
117 examples) are included in a single file. We use Hierarchical Data Format 5 (HDF5) to store the raw
118 waveforms (Folk et al., 2011). Each multi-component waveform example is indexed by a lookup key.
119 For all datasets, the required parameter *‘trace_name’* is used as the lookup key. The labels/metadata

¹See the Data and Resources for the link to the package.

120 associated with each training example are then stored in a simple table-structure (.csv). To ensure com-
121 patibility across datasets, metadata parameter names should follow a common naming schema ‘CATE-
122 GORY_PARAMETER_UNIT’ where: category defines the object which the parameter describes (i.e.,
123 path, source, station, trace); parameter describes the provided information e.g. latitude or longitude;
124 and unit provides the unit of measurement e.g., m, cm, s, counts, samples²

125 Where several entries are required, such as trace start time and station name and location, such a
126 data structure leaves the freedom to include additional specialised metadata only available for selected
127 datasets. The metadata information is read into memory with the popular, high-level data-analysis
128 library Pandas (Reback et al., 2020). With such a format, users can easily create their own custom
129 pipelines to query and extract metadata information associated with the waveforms. Providing a common
130 framework for data storage is key to any proposed benchmarking works. Imposing restrictions on both
131 the format and naming schema ensures that any newly defined parameters are still standardised across
132 datasets. This greatly aids extensibility and comparability across datasets. Data throughput can be
133 a major factor in the efficiency of training and application of ML models. SeisBench therefore introduces
134 additional performance optimizations to the data structure that enhance IO read/write speed.

135 Once a dataset has been converted to the SeisBench format, it is integrated into the SeisBench API
136 by extending the base dataset interface, providing a unique class for the dataset. Ordering the datasets
137 into a class-based hierarchy naturally reflects the dataset format. Common operations such as filtering
138 metadata and obtaining waveforms are all available via the base dataset interface. Further individual
139 properties of each dataset can then be encapsulated in the dataset class. Tools are available to help
140 scientists to convert their own datasets into benchmark datasets and contribute them to the SeisBench
141 repository, if desired.

142 **Providing a common endpoint for benchmark datasets**

143 We have converted a range of seismological benchmark datasets (Table 1; Figure 3) into the SeisBench
144 data format. These datasets contain various types of seismic arrivals from local to global scales (Figure
145 4). All the datasets were either compiled from publicly available seismic data and metadata, or were
146 directly converted from a published benchmark dataset from the literature. SeisBench thus provides
147 easy access to data and model interfaces. All users have to do upon installation of the package is to
148 instantiate their preferred data/model object; the data will then be downloaded and cached for repeat
149 use. Within each benchmark dataset, training, validation, and testing splits are pre-defined to reduce
150 variability of benchmark comparisons resulting from randomness or different choices for dataset splitting
151 approaches. Of course, it remains possible to define custom splits for specialized applications. Here,
152 we summarise the benchmark datasets integrated into the first release of SeisBench. The benchmark

²An example of some of the more typically encountered metadata parameters for SeisBench datasets, and how they would be named in the SeisBench format, can be found in the Data Appendix (Table A1).

153 datasets can be separated into two groups, datasets that are missing some common metadata such as
154 station location information, and those that contain all typical metadata information such as the station
155 location and source parameters. Table 1, and Figure 3 and 4 generally only show those datasets of the
156 first group, where all the common metadata are present. The following dataset descriptions provide
157 further information on the included metadata.

158

159 ETHZ

160 The ETHZ benchmark dataset is a manually compiled dataset for SeisBench. It contains local to re-
161 gionally recorded seismicity throughout Switzerland and neighbouring border regions. The data are
162 recorded on the publicly available networks: 8D; C4; CH; S; XT, operated by the Swiss Seismological
163 Service (SED) at ETH Zurich. To construct this dataset, we obtained both the waveform recordings and
164 the corresponding metadata information via SED's FDSN web service ([http://www.seismo.ethz.ch/
165 de/research-and-teaching/products-software/fdsn-web-services/](http://www.seismo.ethz.ch/de/research-and-teaching/products-software/fdsn-web-services/)). Any detected seismic event
166 from this network has had the phases manually labelled, including the discrimination of first, and later
167 phases (e.g. Pn vs. Pg). In addition to the typical phase identification, the magnitude and polarity
168 information is also available. In total, there are 57 metadata variables available for this dataset. We
169 select all $M > 1.5$ events from the period of 2013 - 2020 for integration. In total there are 2,231 events
170 containing 36,743 waveform examples. The traces are all in raw counts.

171 We split training examples for this dataset into training, validation, and testing example splits by
172 setting all events before August 1st 2019 as training examples (61.6%), all events between this date and
173 the 4th September 2019 are set as the validation split (9.9%), and all the remaining events later than this
174 date are the testing split (28.5%). Please note that the validation set can also be called the development
175 set. These terms are interchangeably used throughout the literature.

176

177 GEOFON

178 The GEOFON monitoring service acquires and analysis waveforms from over 800, globally distributed
179 seismic stations worldwide. The GEOFON benchmark dataset has been compiled from these recordings.
180 It is a teleseismic dataset which includes 2270 events containing $\sim 275,000$ waveform examples occurring
181 between 2009 - 2013. Events have been picked automatically initially, with manual analysis and onset
182 re-picking performed routinely whenever necessary to improve the location quality. The magnitudes
183 range from $\sim M 2 - 9$. With the bulk of events compromising intermediate to large events ($M 5-7$; Figure
184 4). Any regional events with smaller magnitudes are predominantly from the regions of Europe and
185 northern Chile. 54 metadata variables are included with this dataset, the trace units are in raw counts.

186 For the GEOFON dataset, please note the varying class distributions of picked phase types for this
187 dataset. For local and near-regional events S onsets have been picked and for a small fraction both Pn

188 and Pg are included. For teleseismic events, almost no S onsets have been picked. Depth phases have
189 been picked occasionally but not comprehensively

190 For the training, validation and testing splits, we set all events occurring before 1st November 2012 as
191 training examples (58.6%), all events between this date and 15th March 2013 as the validation examples
192 (10.1%), and any remaining events past this date as the testing examples (31.3%).

193

194 INSTANCE

195 The INSTANCE benchmark dataset (Michellini et al., 2021) comprises ~ 1.3 million regional 3-component
196 waveforms from the Italian region, containing $\sim 50,000$ earthquakes M 0 – 6.5 and also including $\sim 130,000$
197 noise examples. Within SeisBench, we provide separate access to the individual partitions of this dataset.
198 The noise examples and signal examples are available as their own distinct dataset; the seismic events are
199 further subdivided into datasets with waveforms in counts, and with waveforms in ground motion units.
200 A combined dataset containing all noise examples and waveform examples in counts is also available.
201 A total of 115 metadata variables are provided. In addition to the standard metadata variables, this
202 dataset includes a rich set of derived metadata, e.g. peak ground acceleration and velocity, assigned pick
203 label uncertainty in seconds.

204 The training, validation, and testing sets are performed by randomly selecting 'event-wise' for this
205 dataset. All waveform examples belonging to the same event are, therefore, in the same split group.
206 The final proportion of waveform examples for each class are 60.3% for training, 10% for validation, and
207 29.7% for testing respectively.

208

209 Iquique

210 The Iquique benchmark dataset is a benchmark dataset of locally recorded seismic arrivals throughout
211 northern Chile originally used in training the deep learning picker in Woollam et al. (2019). It contains
212 13,400 waveform examples with 13,327 manual P-phase picks and 11,361 manual S-phase picks. All
213 waveform units are in raw counts, there are 23 metadata variables associated with this dataset.

214 For this dataset, the training, validation and testing splits are selected through randomly sampling
215 the training examples, returning 60%, 30% and 10% for the training, validation, and testing splits
216 respectively.

217 LenDB

218 The LenDB benchmark dataset (Magrini et al., 2020) is a published benchmark dataset containing local
219 earthquakes recorded across a global set of 1487 broad-band and very broad-band seismic stations. It
220 comprises ~ 1.25 million waveforms. The dataset is split into 629,095 local earthquake examples and
221 615,847 noise examples. The data were processed using a bandpass filter between 0.1 - 5 Hz and the
222 instrument response was deconvolved to convert the recordings into physical units of velocity. Unlike the

223 other datasets, only automatic P-phase picks are provided for LenDB. In total there are 23 metadata
224 variables for this dataset.

225 The training, validation, testing split is performed by selecting all examples with waveform start
226 times before 16th January 2017 as training examples (60%). Any examples between this date and the
227 16th August 2017 form the validation split (9.5%), and the remaining examples past this date form the
228 test split (30.5%).

229

230 SCEDC

231 The Southern Californian Earthquake Data Centre (SCEDC) benchmark dataset has been constructed
232 from publicly available waveform data (SCEDC, 2013). The waveforms and associated metadata are
233 obtained via the Seismic Transfer Programme (STP) client (SCEDC, 2010). For the obtained seismic
234 arrivals, all events have been manually picked. We select all publicly available recordings of seismic
235 events in the Southern Californian Seismic Network, over the period 2000 - 2020. Only local recordings
236 of seismic events ($\sim M -1 - 7$) are included, with source to station paths spanning up to a maximum
237 distance of ~ 200 km. The dataset comprises ~ 8 million waveform examples, which contain ~ 7.5 million
238 P-phases and ~ 4.3 million S-phases. This dataset also contains a range of seismic instrument types
239 including: extremely short period, short period, very broadband, broadband, intermediate band and
240 long period instruments - both single and 3-component channels are also present. Units for the examples
241 are raw counts.

242 The split for this dataset is set randomly, with 60%, 10%, and 30% of the data comprising the
243 training, development, and testing splits respectively. For the magnitude metadata information, please
244 note the increase of $M = 0$ in events in comparison to the overall trend (Figure 4) which suggests some
245 data cleaning is still required for this dataset for the purposes of magnitude prediction.

246

247 STEAD

248 The STanford EArthquake Dataset (STEAD; Mousavi, Sheng, Zhu and Beroza, 2019) published bench-
249 mark dataset, contains a range of local seismic signals – both earthquake and non-earthquake – along
250 with noise examples. The dataset includes ~ 1.2 million waveforms, of which $\sim 200,000$ are noise examples
251 and the remaining contain seismic arrivals from $\sim 450,000$ earthquakes ($\sim M -0.5 - 8$). The units for the
252 waveform examples are raw counts and there are 40 metadata variables associated with this event.

253 For the split, we use the same test set as defined in Mousavi et al. (2020) which randomly set 10%
254 of the examples as testing examples, we then add a validation set by randomly sampling from the re-
255 maining samples. The final ratios of the training, validation, and testing split are again 60%, 30%, 10%
256 respectively.

257

258 The following datasets include cases where the publicly available waveform data, along with corre-
259 sponding metadata was available for training ML models, but some common metadata is missing.

260

261 NEIC

262 The National Earthquake Information Centre (NEIC; Yeck et al., 2021) published benchmark dataset
263 comprises ~ 1.3 million seismic phase arrivals with global source-station paths. As information on the
264 trace start-time and station is missing for this dataset, it is stored in the SeisBench format, but without
265 this normally required information.

266 For the training, development and testing split, the original publication presented randomly sampled
267 splits, based on event-id. This random splitting approach is implemented in the SeisBench conversion of
268 this dataset, again at 60%, 10%, and 30% for the training, development, and testing examples respec-
269 tively.

270

271 There are additional datasets integrated into SeisBench which were originally used in training notable
272 deep learning algorithms in seismology. Typically, the waveforms for these datasets were already pre-
273 processed for training, including windowing and labelling, so the original station metadata for each
274 training example is unavailable for these datasets. As many of the datasets also use picked waveforms
275 from the SCEDC network, this results in potential common overlap between the following listed datasets,
276 for both metadata parameters and waveforms. The only differences being potentially different metadata
277 variables across datasets (e.g. picked phase labels, vs. first motion labels).

278 The deep learning training datasets converted into SeisBench format include: the 'GPD' training
279 dataset (Ross, Meier, Hauksson and Heaton, 2018) containing 4,773,750 examples of 4s waveforms,
280 sampled at 100 Hz; the 'Ross2018JGRFM' dataset used for training the deep learning-based first motion
281 polarity detection routine in the Ross, Meier and Hauksson (2018) study, containing 6 s Z-component
282 waveform samples from 100 Hz instruments; the 'Ross2018JGRPick' dataset used for training the deep
283 learning-based picker presented in the same work; The 'Meier2019JGR' dataset, which contains the S.
284 Californian component of the training examples from the Meier et al. (2019) work.

285 Models

286 The SeisBench *model* interface is an extensible framework which encompasses the application of all types
287 of models to seismic data. It is designed to be generalizable to arbitrary seismic tasks which operate
288 on waveform data. A range of deep learning models from the literature are provided through SeisBench
289 (Table 2). All deep learning models are integrated with the PyTorch framework (Paszke et al., 2017).
290 Where possible, models integrated into SeisBench have the corresponding weights from the original

291 training procedure integrated. We also provide weights for each of the models trained on each of the
292 included datasets (see the companion paper to this work, Münchmeyer and 12 coauthors (n.d.)).

293 **Initially integrated models**

294 The initial set of models integrated into SeisBench are listed below, where the acronyms CNN and RNN
295 relate to Convolutional Neural Network, and Recurrent Neural Network respectively. For a more detailed
296 description, refer to (Münchmeyer and 12 coauthors, n.d.).

- 297 • BasicPhaseAE (Woollam et al., 2019), basic CNN U-Net, initially applied to regional aftershock
298 sequence in Chile.
- 299 • CRED (Mousavi, Zhu, Sheng and Beroza, 2019), CNN-RNN Earthquake Detector, initially trained
300 on 500,000 training signal and noise examples from Northern California.
- 301 • DPP (Soto and Schurr, 2021), DeepPhasePick, is a combination of a CNN for phase detection
302 and two RNNs for onset time determination. Like BasicPhaseAE, the networks were designed for
303 detecting and picking local events, with an initial application on a regional seismic network in
304 Chile.
- 305 • EQT (Mousavi et al., 2020), EarthQuake Transformer, an Attention-based Transformer Network
306 to both detect and pick events.
- 307 • GPD (Ross, Meier, Hauksson and Heaton, 2018) Generalised Phase Detection, CNN algorithm to
308 detect seismic phases.
- 309 • PhaseNet (Zhu and Beroza, 2019), CNN autoencoder algorithm, adapts the U-Net segmentation
310 framework to the 1D problem of classifying seismic phases.

311 **Training data generation pipeline**

312 A common task for training ML models in seismology is building data generation pipelines. First, some
313 pre-processing is usually done; for example, traces need to be truncated to the correct length and possibly
314 normalized, labels need to be encoded. Furthermore, often it is beneficial to augment the data to increase
315 the variability on training examples, for example by adding noise to the waveforms. To standardize this
316 task, reduce the required coding amount and reduce errors in the training pipeline, SeisBench provides
317 the *generate* API (cf. Figure 1).

318 The *generate* API provides individual processing blocks, e.g., window selection, label definition, or
319 normalization, which can be combined into a data generation pipeline in a flexible way. While many
320 standard augmentations are already implemented, custom routines can be added easily. As the *generate*

321 API only relies on the abstract *data* API, the same set of augmentations can be applied to any SeisBench
322 compatible dataset with minimal changes in the code. In addition, since the *generate* API is integrated
323 with PyTorch, it can facilitate efficient data generation with PyTorch’s built-in multi-processing.

324 **Example workflows - Using SeisBench benchmark datasets and** 325 **models**

326 Here we highlight how the features and functionality provided through SeisBench can support users with
327 their tasks, from practitioners just looking to use an ML model to experts wishing to conduct extensive,
328 in-depth, comparison and benchmarking pipelines.

329 **Workflow 1 - Use pre-trained models for picking new seismic streams**

330 This workflow is relevant for practitioners who seek to leverage ML techniques on seismic data, but do
331 not necessarily have the in-depth domain knowledge to do this through ML frameworks. This example
332 demonstrates how to pick seismic waveforms with two leading, pre-trained models (EQT and GPD) via
333 the SeisBench API. The commands to do this are displayed in Figure 5. The high-level functionality
334 allows users to apply ML models to seismic data with just a few commands. If not previously downloaded,
335 the pre-trained model weights are downloaded and subsequently cached for repeat use. The *annotate*
336 and *classify* methods of the SeisBench models integrate with *stream* objects from the *obspy* package
337 (Beyreuther et al., 2010), widely used within the seismological community. We omit the plotting code
338 for brevity. Users can easily expand upon this example workflow to conduct seismic detection and picking
339 pipelines. In terms of computational performance, we test the EQTransformer implementation on a K80
340 GPU and *annotate* 24 hours of 100 Hz data from a single station in 6 s. Scaling this process results in a
341 months worth of data being labelled in ~3 minutes.

342 **Workflow 2 - Training models**

343 **Training a deep learning model**

344 For those wishing to train a deep learning model, Figure 6 provides a run through of how this workflow
345 can be built in SeisBench. This workflow highlights how the *data*, *generate*, and *model* modules combine
346 to help users perform all the typical tasks required in such a pipeline. Any loading of the required models
347 and data is performed initially. In this example, we train PhaseNet on the INSTANCE dataset. Once
348 the dataset and model are loaded, the *generate* module can be used to perform typical pre-processing
349 and data augmentation steps on the waveforms. The generator object accepts a suite of augmentations
350 which will be applied to each batch during training. In this example, we randomly window the waveforms,

351 normalise the amplitudes using the maximum amplitude present in the window, change the datatype to
352 32bit floats, finally creating a probabilistic vector representation of P-picks, S-picks, and noise examples
353 in the waveform. These steps can be achieved in 10 lines of code through SeisBench (see the *Preprocessing*
354 *and augmentations* code block, Figure 6). The waveforms following processing are displayed in Figure 6.
355 The augmented waveform data then form a training sample for PhaseNet. We also show the standard
356 PyTorch syntax to iterate through a DataLoader object and train the model as the last step (see the
357 *Train* code block, Figure 6).

358 **Transfer learning**

359 Rather than train a new model from scratch, transfer learning forms another common workflow users
360 may require. Transfer learning, involves using a pre-trained model, initially trained for some given task
361 - for example detecting seismic phases on a regional scale throughout S. California - and subsequently
362 training the model to solve a related task - such as detecting teleseismic arrivals. This is often a useful
363 as the knowledge learned during the initial training phase results in relatively less data being required
364 to optimize the model for the new task.

365 The modular nature of the API means that to switch any dataset or model for another, all that is
366 required is to change data or model imported (indicated by the dashed lines in Figure 6). So, to load
367 a pre-trained version of a given model, all users have to do is call the *from_pretrained* method. The
368 syntax to perform this step is also displayed in workflow 1. Datasets can also be swapped easily. For
369 the purposes of this example, any dataset containing P-, and S-picks could be loaded in place of the
370 INSTANCE dataset in workflow 2, and the training would then be performed on this alternative dataset,
371 using the PhaseNet model initially trained on regional seismic waveforms in California as initialization
372 for the training.

373 **Workflow 3 - Benchmark differing models across differing datasets**

374 Beyond training for a single model or dataset, SeisBench allows for comparison pipelines to be easily
375 constructed. Having an objective measure of the performance of newly proposed algorithms against
376 current state-of-the-art routines is fundamental to progress in any field, and standard procedure in
377 traditional ML domains such as image recognition. As ML is a recent adoption within seismology, it
378 could be argued that this step has not yet been carried out extensively. A detailed benchmarking study
379 of various published ML picking models was carried out by us with the SeisBench framework and is
380 presented with the companion paper to this work (Münchmeyer and 12 coauthors, n.d.). The code used
381 for this benchmark study is made available and can serve as a template for future benchmarking studies³.

³Available at <https://github.com/seisbench/pick-benchmark>

382 Extensibility

383 The SeisBench API is published with an open-source license (GPLv3). The software is designed to be
384 extensible, and we encourage the seismological community to contribute. If users wish to integrate their
385 own benchmark datasets or models to the package for public download, we ask that they get in touch
386 with the project through GitHub (<https://www.github.com/seisbench/seisbench>); where further
387 information on the contribution guidelines can be found. In particular, we encourage inclusion of already
388 published models and datasets. The code-base has extensive test coverage to reduce the risk of coding
389 errors.

390 With the picking and detection problems having been widely explored in recent years with ML
391 approaches, more complex problems are now being tackled with these techniques. We envisage that
392 the models incorporated into SeisBench will expand to include such tasks. For example, hypocentre
393 determination, source parameter estimation, etc., can all be constructed with SeisBench. All that is
394 required is that the labels for a supervised learning task are present in the metadata. Once the state-of-
395 the-art ML models for a given task are available in SeisBench - as shown with the picking example above
396 - the major advantages of integrating new models within this framework become apparent. The initial
397 processing routine set up for a model can be directly used to compare against existing state-of-the-art
398 models. This ease of testing will hopefully promote further innovation of ML in seismology.

399 Conclusions

400 We have developed SeisBench as an open-source Python package, built to aid users in their application
401 of ML techniques to seismic data. It minimizes common barriers to development for both practitioners
402 looking to apply ML methods to seismic tasks, and experts who wish to benchmark and train leading
403 algorithms. The software provides access to recently published benchmark datasets for machine learning
404 in seismology, downloadable and accessible through a common interface. SeisBench extends this concept
405 to provide a common access point to ML models, with state-of-the-art models and corresponding weights
406 for seismic tasks directly integrated. We provide access to a range of picking models from the literature
407 in the first iteration of the software but the framework is applicable for many seismological tasks based
408 on waveform analysis such as location and magnitude estimation. By tackling some of the common
409 bottlenecks encountered when developing ML algorithms, we hope that SeisBench will help practitioners
410 iterate and deploy their models, advancing the development of the next generation of ML techniques
411 within seismology.

412 Acknowledgements

413 We thank the Impuls- und Vernetzungsfonds of the HGF to support the REPORT-DL project under
414 the grant agreement ZT-I-PF-5-53. We use PyTorch (Paszke et al., 2017) for integrating deep learning
415 models into the package. JM acknowledges the support of the Helmholtz Einstein International Berlin
416 Research School in Data Science (HEIBRiDS). This work was also partially supported by the project
417 INGV Pianeta Dinamico 2021 Tema 8 SOME (CUP D53J1900017001) funded by Italian Ministry of
418 University and Research “Fondo finalizzato al rilancio degli investimenti delle amministrazioni centrali
419 dello Stato e allo sviluppo del Paese, legge 145/2018”. We thank the reviewers S. Mostafa Mousavi and
420 Steve Hicks for their positive, detailed reviews which greatly helped improve the manuscript.

421 We would also like to thank the authors of the original benchmarking and model papers, who made
422 publicly available either benchmark datasets, or original model weights. Open-source development is an
423 important component of advancing research and SeisBench only works as a tool with these models and
424 datasets openly accessible.

425 Data and Resources

426 All data used in this paper either come from published sources listed in the references, or are com-
427 piled from publicly available seismic recordings. Further information on how each individual dataset
428 obtained, or accessed any waveform data can be found in the *Data - Standardising access to Bench-*
429 *mark datasets* section. The source code for SeisBench is available through GitHub [https://www.](https://www.github.com/seisbench/seisbench)
430 [github.com/seisbench/seisbench](https://www.github.com/seisbench/seisbench), with the associated documentation also hosted at the following
431 link <https://seisbench.readthedocs.io/en/latest/>.

432 Declaration of Competing Interests

433 The authors declare no competing interests.

434 References

- 435 Abadi, M., Barham, P., Chen, J., Chen, Z., Davis, A., Dean, J., Devin, M., Ghemawat, S., Irving, G.,
436 Isard, M. et al. (2016), Tensorflow: A system for large-scale machine learning, *in* ‘12th {USENIX}
437 symposium on operating systems design and implementation ({OSDI} 16)’, pp. 265–283.
- 438 Akbik, A., Bergmann, T., Blythe, D., Rasul, K., Schweter, S. and Vollgraf, R. (2019), Flair: An easy-
439 to-use framework for state-of-the-art nlp, *in* ‘NAACL 2019, 2019 Annual Conference of the North
440 American Chapter of the Association for Computational Linguistics (Demonstrations)’, pp. 54–59.
- 441 AlpArray Seismic Network (2014), ‘Eastern alpine seismic investigation (easi) - alparray complimentary
442 experiment’.
- 443 **URL:** <http://networks.seismo.ethz.ch/networks/xt/>
- 444 Beyreuther, M., Barsch, R., Krischer, L., Megies, T., Behr, Y. and Wassermann, J. (2010), ‘Obspy: A
445 python toolbox for seismology’, *Seismological Research Letters* **81**(3), 530–533.
- 446 CERN (2016), ‘Cern seismic network’.
- 447 **URL:** <http://networks.seismo.ethz.ch/networks/c4/>
- 448 Chollet, F. et al. (2015), ‘Keras’.
- 449 **URL:** <https://github.com/fchollet/keras>
- 450 Deng, J., Dong, W., Socher, R., Li, L.-J., Li, K. and Fei-Fei, L. (2009), Imagenet: A large-scale hier-
451 archical image database, *in* ‘2009 IEEE conference on computer vision and pattern recognition’, Ieee,
452 pp. 248–255.
- 453 Deng, L. (2012), ‘The mnist database of handwritten digit images for machine learning research’, *IEEE*
454 *Signal Processing Magazine* **29**(6), 141–142.
- 455 Dokht, R. M., Kao, H., Visser, R. and Smith, B. (2019), ‘Seismic event and phase detection using
456 time–frequency representation and convolutional neural networks’, *Seismological Research Letters*
457 **90**(2A), 481–490.
- 458 Folk, M., Heber, G., Koziol, Q., Pourmal, E. and Robinson, D. (2011), An overview of the hdf5 technology
459 suite and its applications, *in* ‘Proceedings of the EDBT/ICDT 2011 Workshop on Array Databases’,
460 pp. 36–47.
- 461 Go, A., Bhayani, R. and Huang, L. (2009), ‘Twitter sentiment classification using distant supervision’.
- 462 **URL:** <http://help.sentiment140.com/home>
- 463 Király, F. J., Löning, M., Blaom, A., Guecioueur, A. and Sonabend, R. (2021), ‘Designing machine
464 learning toolboxes: Concepts, principles and patterns’, *arXiv preprint arXiv:2101.04938* .

465 Kong, Q., Allen, R. M., Schreier, L. and Kwon, Y.-W. (2016), ‘Myshake: A smartphone seismic network
466 for earthquake early warning and beyond’, *Science advances* **2**(2), e1501055.

467 Li, Z., Meier, M.-A., Hauksson, E., Zhan, Z. and Andrews, J. (2018), ‘Machine learning seismic wave
468 discrimination: Application to earthquake early warning’, *Geophysical Research Letters* **45**(10), 4773–
469 4779.

470 Lomax, A., Michelini, A. and Jozinović, D. (2019), ‘An investigation of rapid earthquake characterization
471 using single-station waveforms and a convolutional neural network’, *Seismological Research Letters*
472 **90**(2A), 517–529.

473 Magrini, F., Jozinović, D., Cammarano, F., Michelini, A. and Boschi, L. (2020), ‘Local earthquakes detec-
474 tion: A benchmark dataset of 3-component seismograms built on a global scale’, *Artificial Intelligence
475 in Geosciences* **1**, 1–10.

476 Meier, M.-A., Ross, Z. E., Ramachandran, A., Balakrishna, A., Nair, S., Kundzicz, P., Li, Z., Andrews, J.,
477 Hauksson, E. and Yue, Y. (2019), ‘Reliable real-time seismic signal/noise discrimination with machine
478 learning’, *Journal of Geophysical Research: Solid Earth* **124**(1), 788–800.

479 Michelini, A., Cianetti, S., Gaviano, S., Giunchi, C., Jozinovic, D. and Lauciani, V. (2021), ‘Instance-the
480 italian seismic dataset for machine learning’, *Earth System Science Data Discussions* pp. 1–47.

481 Mousavi, S. M. and Beroza, G. C. (2020), ‘A machine-learning approach for earthquake magnitude
482 estimation’, *Geophysical Research Letters* **47**(1), e2019GL085976.

483 Mousavi, S. M., Ellsworth, W. L., Zhu, W., Chuang, L. Y. and Beroza, G. C. (2020), ‘Earthquake trans-
484 former—an attentive deep-learning model for simultaneous earthquake detection and phase picking’,
485 *Nature communications* **11**(1), 1–12.

486 Mousavi, S. M., Sheng, Y., Zhu, W. and Beroza, G. C. (2019), ‘Stanford earthquake dataset (stead): A
487 global data set of seismic signals for ai’, *IEEE Access* **7**, 179464–179476.

488 Mousavi, S. M., Zhu, W., Sheng, Y. and Beroza, G. C. (2019), ‘Cred: A deep residual network of
489 convolutional and recurrent units for earthquake signal detection’, *Scientific reports* **9**(1), 1–14.

490 Münchmeyer, J. and 12 coauthors (n.d.), ‘Which picker fits my data? a quantitative evaluation of
491 deeplearning based seismic pickers’.
492 **URL:** [https://arxiv.org/.](https://arxiv.org/)

493 Münchmeyer, J., Bindi, D., Leser, U. and Tilmann, F. (2021 a), ‘Earthquake magnitude and location
494 estimation from real time seismic waveforms with a transformer network’, *Geophysical Journal Inter-
495 national* **226**(2), 1086–1104.

496 Münchmeyer, J., Bindi, D., Leser, U. and Tilmann, F. (2021*b*), ‘The transformer earthquake alerting
 497 model: a new versatile approach to earthquake early warning’, *Geophysical Journal International*
 498 **225**(1), 646–656.

499 Pardo, E., Garfias, C. and Malpica, N. (2019), ‘Seismic phase picking using convolutional networks’,
 500 *IEEE Transactions on Geoscience and Remote Sensing* **57**(9), 7086–7092.

501 Paszke, A., Gross, S., Chintala, S., Chanan, G., Yang, E., DeVito, Z., Lin, Z., Desmaison, A., Antiga, L.
 502 and Lerer, A. (2017), ‘Automatic differentiation in pytorch’.

503 Pedregosa, F., Varoquaux, G., Gramfort, A., Michel, V., Thirion, B., Grisel, O., Blondel, M., Pretten-
 504 hofer, P., Weiss, R., Dubourg, V. et al. (2011), ‘Scikit-learn: Machine learning in python’, *Journal of*
 505 *machine learning research* **12**(Oct), 2825–2830.

506 Perol, T., Gharbi, M. and Denolle, M. (2018), ‘Convolutional neural network for earthquake detection
 507 and location’, *Science Advances* **4**(2), e1700578.

508 Reback, J., McKinney, W., Den Van Bossche, J., Augspurger, T., Cloud, P., Klein, A., Roeschke, M.,
 509 Hawkins, S., Tratner, J., She, C. et al. (2020), ‘pandas-dev/pandas: Pandas 1.0. 3’, *Zenodo* .

510 Ross, Z. E., Meier, M.-A. and Hauksson, E. (2018), ‘P wave arrival picking and first-motion polarity
 511 determination with deep learning’, *Journal of Geophysical Research: Solid Earth* **123**(6), 5120–5129.

512 Ross, Z. E., Meier, M.-A., Hauksson, E. and Heaton, T. H. (2018), ‘Generalized seismic phase detection
 513 with deep learning’, *Bulletin of the Seismological Society of America* **108**(5A), 2894–2901.

514 SCEDC (2010), ‘Seismic transfer program (version 1.4.1)’.
 515 **URL:** <https://scedc.caltech.edu/data/stp/>

516 SCEDC (2013), ‘Southern california earthquake data center. caltech. dataset’.

517 Soto, H. and Schurr, B. (2021), ‘DeepPhasePick: a method for detecting and picking seismic phases
 518 from local earthquakes based on highly optimized convolutional and recurrent deep neural networks’,
 519 *Geophysical Journal International* **227**(2), 1268–1294.

520 Swiss Seismological Service (SED) At ETH Zurich (1983), ‘National seismic networks of switzerland’.
 521 **URL:** <http://networks.seismo.ethz.ch/networks/ch/>

522 Swiss Seismological Service (SED) At ETH Zurich (2005), ‘Temporary deployments in switzerland asso-
 523 ciated with aftershocks and other seismic sequences’.
 524 **URL:** <http://networks.seismo.ethz.ch/networks/8d/>

525 Swiss Seismological Service (SED) At ETH Zurich (2008), ‘Seismology at school program, eth zurich’.
 526 **URL:** <http://networks.seismo.ethz.ch/networks/s/>

- 527 Valentine, A. P. and Trampert, J. (2012), ‘Data space reduction, quality assessment and search-
528 ing of seismograms: autoencoder networks for waveform data’, *Geophysical Journal International*
529 **189**(2), 1183–1202.
530 **URL:** <http://dx.doi.org/10.1111/j.1365-246X.2012.05429.x>
- 531 van den Ende, M. P. and Ampuero, J.-P. (2020), ‘Automated seismic source characterization using deep
532 graph neural networks’, *Geophysical Research Letters* **47**(17), e2020GL088690.
- 533 Wang, J. and Teng, T.-l. (1997), ‘Identification and picking of s phase using an artificial neural network’,
534 *Bulletin of the Seismological Society of America* **87**(5), 1140–1149.
- 535 Wang, J., Xiao, Z., Liu, C., Zhao, D. and Yao, Z. (2019), ‘Deep learning for picking seismic arrival times’,
536 *Journal of Geophysical Research: Solid Earth* **124**(7), 6612–6624.
- 537 Woollam, J., Rietbrock, A., Bueno, A. and De Angelis, S. (2019), ‘Convolutional neural network for
538 seismic phase classification, performance demonstration over a local seismic network’, *Seismological*
539 *Research Letters* **90**(2A), 491–502.
- 540 Yeck, W. L., Patton, J. M., Ross, Z. E., Hayes, G. P., Guy, M. R., Ambruz, N. B., Shelly, D. R., Benz,
541 H. M. and Earle, P. S. (2021), ‘Leveraging deep learning in global 24/7 real-time earthquake monitoring
542 at the national earthquake information center’, *Seismological Society of America* **92**(1), 469–480.
- 543 Zhou, Y., Yue, H., Kong, Q. and Zhou, S. (2019), ‘Hybrid event detection and phase-picking algorithm
544 using convolutional and recurrent neural networks’, *Seismological Research Letters* **90**(3), 1079–1087.
- 545 Zhu, W. and Beroza, G. C. (2019), ‘Phasenet: a deep-neural-network-based seismic arrival-time picking
546 method’, *Geophysical Journal International* **216**(1), 261–273.

547 Mailing Addresses

- 548 • jack.woollam@kit.edu
- 549 • munchmej@gfz-potsdam.de
- 550 • tilmann@gfz-potsdam.de
- 551 • andreas.rietbrock@kit.edu
- 552 • dlange@geomar.de
- 553 • saul@gfz-potsdam.de
- 554 • djozinovi@gmail.com
- 555 • alberto.michelini@ingv.it
- 556 • carlo.giunchi@ingv.it
- 557 • tobias.diehl@sed.ethz.ch
- 558 • florian.haslinger@sed.ethz.ch
- 559 • soto@gfz-potsdam.de
- 560 • bornstth@hu-berlin.de

561 List of Figure Captions

- 562 1. Schematic diagram to show the motivation behind SeisBench. SeisBench acts as a unifying frame-
563 work for developing models and applying them to seismic data. The differing packages used
564 for model development, and the differing benchmark dataset formats are represented by vary-
565 ing colours. The *data*, *generate*, and *model* tags highlight the different modules available within
566 SeisBench.
- 567 2. Example of data structure for SeisBench. Waveforms are stored in a HDF5 file, indexed by
568 trace name. The metadata for each waveform example is stored in a table format as a .csv
569 file. The trace name is required as a column, as this is then used as the lookup key to the
570 raw data. This schematic diagram displays the overall concept, with the implementation slightly
571 more complex to optimise performance. For more information see the technical documentation
572 (<https://seisbench.readthedocs.io/en/latest/>).
- 573 3. Benchmark datasets integrated into SeisBench with the initial release of the software; seismic
574 sources are circles, stations are triangle markers. Not shown are some additional datasets which are
575 included in the SeisBench initial release dataset collection, but are either missing source information
576 (NEIC, GPD, Ross2018JGRPick, Ross2018JGRFM, Meier2019JGR), or have minimal number of
577 events for plotting (the local Iquique dataset).
- 578 4. Logarithmic histograms of epicentral distance and magnitude distributions for the datasets with
579 source and station information. For the two-dimensional scatterplot in the last column, all points
580 are plotted with transparency to highlight the overall distribution. The Iquique, NEIC, GPD,
581 Ross2018JGRPick, Ross2018JGRFM, Meier2019JGR datasets are not shown because they are
582 lacking either, magnitude, or source and station location information.
- 583 5. Example code-blocks which download a seismic waveform [1], then loads a pre-trained deep learning
584 picking model and applies the model to predict on the seismic stream using either one of two ML
585 architectures (GPD and EQTransformer) [2]. Resulting picks and characteristic functions from the
586 output probabilities are displayed beneath the code blocks. Characteristic function is abbreviated
587 to "CF". Picks are represented by dotted lines, event detections for the EQT case are the shaded
588 regions. The GPD picker makes a spurious S -pick before the onset of the event but as the original
589 model weights have been incorporated into the pickers to pick on new, unseen data, this example
590 may not be representative of the optimum performance of the respective model architectures, which
591 could be achieved by training on data matched to the application case.
- 592 6. Example code-block with additional schematic diagrams displaying syntax required to perform full
593 training of a deep learning model in SeisBench. PhaseNet is used for training, with the INSTANCE

594 dataset being used as training data. Further workflow examples demonstrating the functionality
595 provided by SeisBench can be found at [https://github.com/seisbench/seisbench/tree/main/](https://github.com/seisbench/seisbench/tree/main/examples)
596 examples.

Tables

Table 1: Overview of the datasets. The noise column indicates the number of dedicated noise traces. Note that it is still possible to extract noise examples from datasets without dedicated noise traces by selecting windows before the first arrival. For distances, the datasets cover local (L, $0 \leq \Delta < 150$ km), regional (R, $150 \leq \Delta < 600$ km), and teleseismic (T, $\Delta > 600$ km) records. The datasets with variable trace length contain considerably more than 60s of data for most examples. f_s denotes the sampling rate, Tr. length denotes the trace length in seconds. When the sampling rate varies within a dataset, the range of sampling rates is listed. The GPD, Ross2018JGRPick, Ross2018JGRFM, Meier2019JGR datasets are omitted from this table because these datasets do not contain source property information. NEIC is included because it is used for the benchmark comparison in Münchmeyer and 12 coauthors (n.d.). The horizontal split in the table separates the benchmark datasets containing regional to local arrivals (top section), and the datasets containing teleseismic arrivals (bottom section).

	Traces	Events	P picks	S picks	Noise	Region	Dist	Tr. length	f_s [Hz]
ETHZ	36,743	2,231	35,227	18,960	0	Switzerland	L/R	variable	100 - 500
INSTANCE	1,291,537	54,008	1,159,249	713,883	132,288	Italy	L/R	120 s	100
Iquique	13,400	409	13,327	11,361	0	N. Chile	L	variable	100
LenDB	1,244,942	303,902	629,095	0	615,847	various	L	27 s	20
SCEDC	8,111,060	378,528	7,571,970	4,364,155	0	S. California	L	variable	40 - 100
STEAD	1,265,657	441,705	1,030,231	1,030,231	235,426	various	L/R	60 s	100
GEOFON	275,274	2,270	284,240	2,847	0	global	R/T	variable	20 - 200
NEIC	1,354,789	137,424	1,025,000	329,789	0	global	R/T	60 s	40

Table 2: Description of the models studied. The number of parameters refers to the total number of trainable parameters. Note that these numbers might deviate slightly from the ones published by the original authors due to differences in the underlying frameworks. For DPP, information delimited by slashes indicate Detector/P-Picker/S-Picker networks. The row "Orig. weights" indicates whether original weights were published and are available in SeisBench. For PhaseNet, weights were published by the authors, but these weights could not straightforwardly be integrated into SeisBench due to technical issues.

	BascicPhaseAE	CRED	DPP	EQT	GPD	PhaseNet
# Params	33,687	293,569	199,731/ 546,081/ 21,181	376,935	1,741,003	23,305
Type	U-Net	CNN-RNN	CNN/RNN/RNN	CNN-RNN- Attention	CNN	U-Net
Training set	N. Chile	S. California	N. Chile	STEAD	S. California	N. California
Orig. weights	N	Y	N	Y	Y	N
Reference	Woollam et al. (2019)	Mousavi, Zhu, Sheng and Beroza (2019)	Soto and Schurr (2021)	Mousavi et al. (2020)	Ross, Meier, Hauksson and Heaton (2018)	Zhu and Beroza (2019)

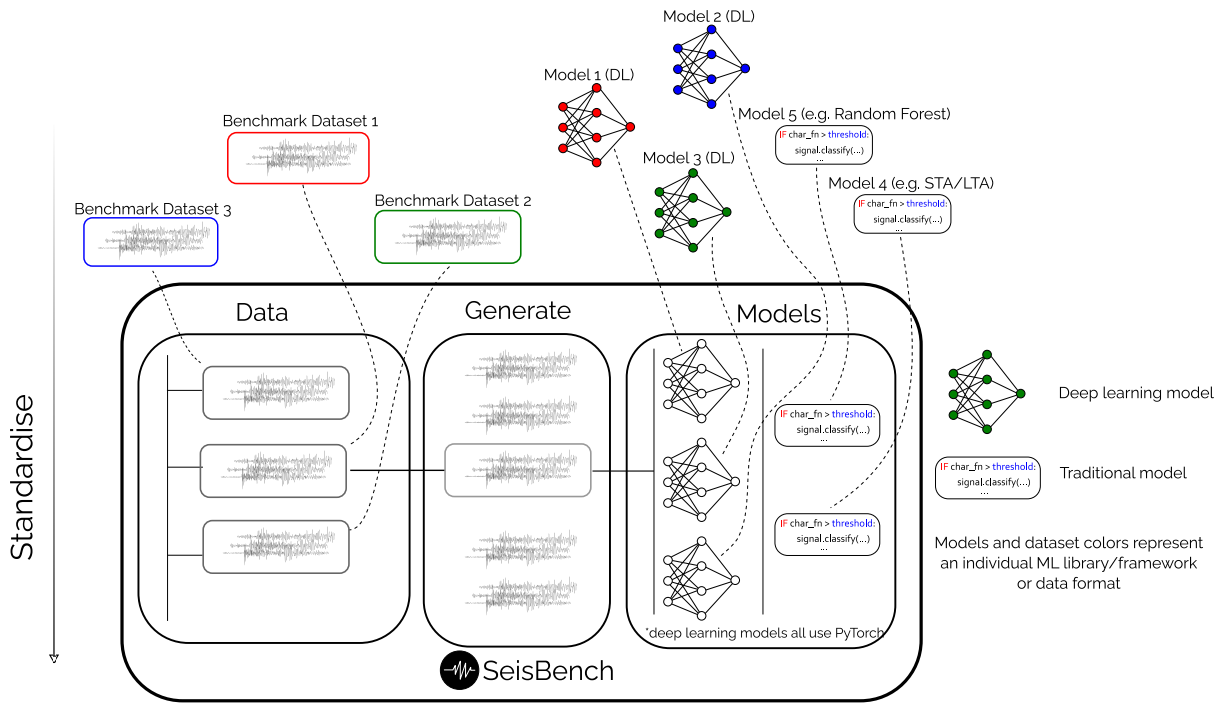


Figure 1: Schematic diagram to show the motivation behind SeisBench. SeisBench acts as a unifying framework for developing models and applying them to seismic data. The differing packages used for model development, and the differing benchmark dataset formats are represented by varying colours. The *data*, *generate*, and *model* tags highlight the different modules available within SeisBench.

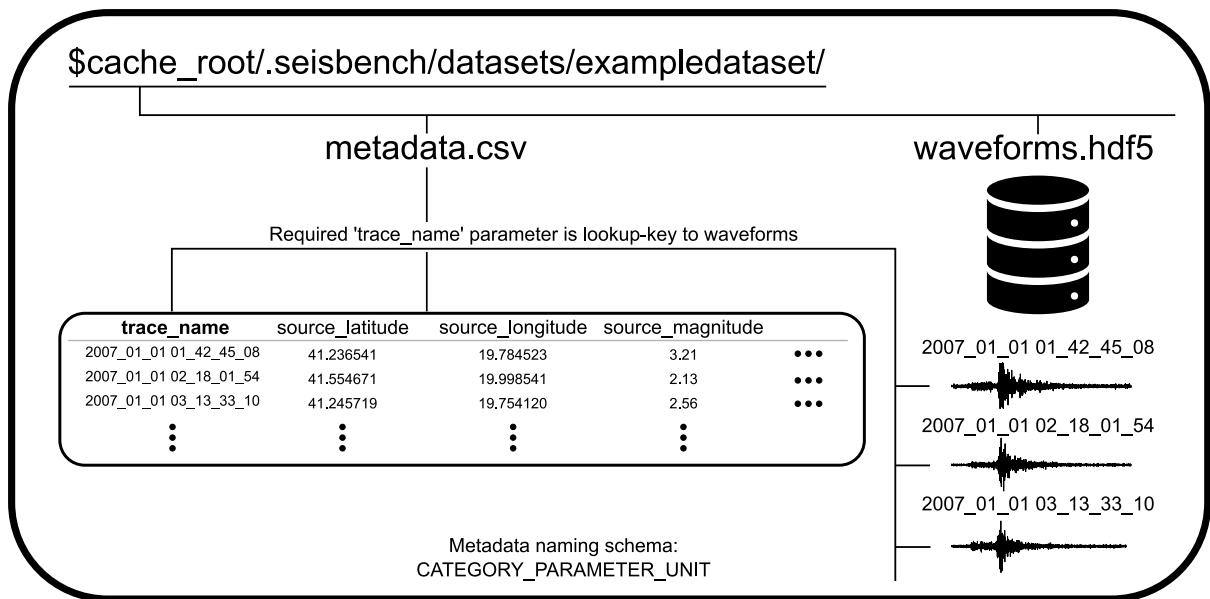


Figure 2: Example of data structure for SeisBench. Waveforms are stored in a HDF5 file, indexed by trace name. The metadata for each waveform example is stored in a table format as a .csv file. The trace name is required as a column, as this is then used as the lookup key to the raw data. This schematic diagram displays the overall concept, with the implementation slightly more complex to optimise performance. For more information see the technical documentation (<https://seisbench.readthedocs.io/en/latest/>).

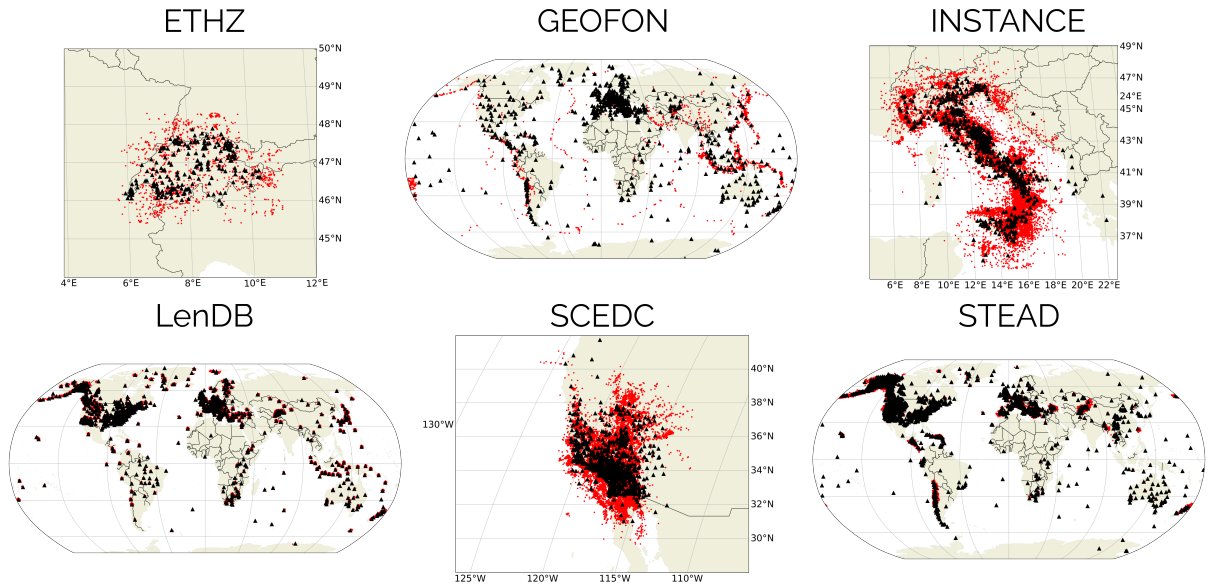


Figure 3: Benchmark datasets integrated into SeisBench with the initial release of the software; seismic sources are circles, stations are triangle markers. Not shown are some additional datasets which are included in the SeisBench initial release dataset collection, but are either missing source information (NEIC, GPD, Ross2018JGRPick, Ross2018JGRFM, Meier2019JGR), or have minimal number of events for plotting (the local Iquique dataset).

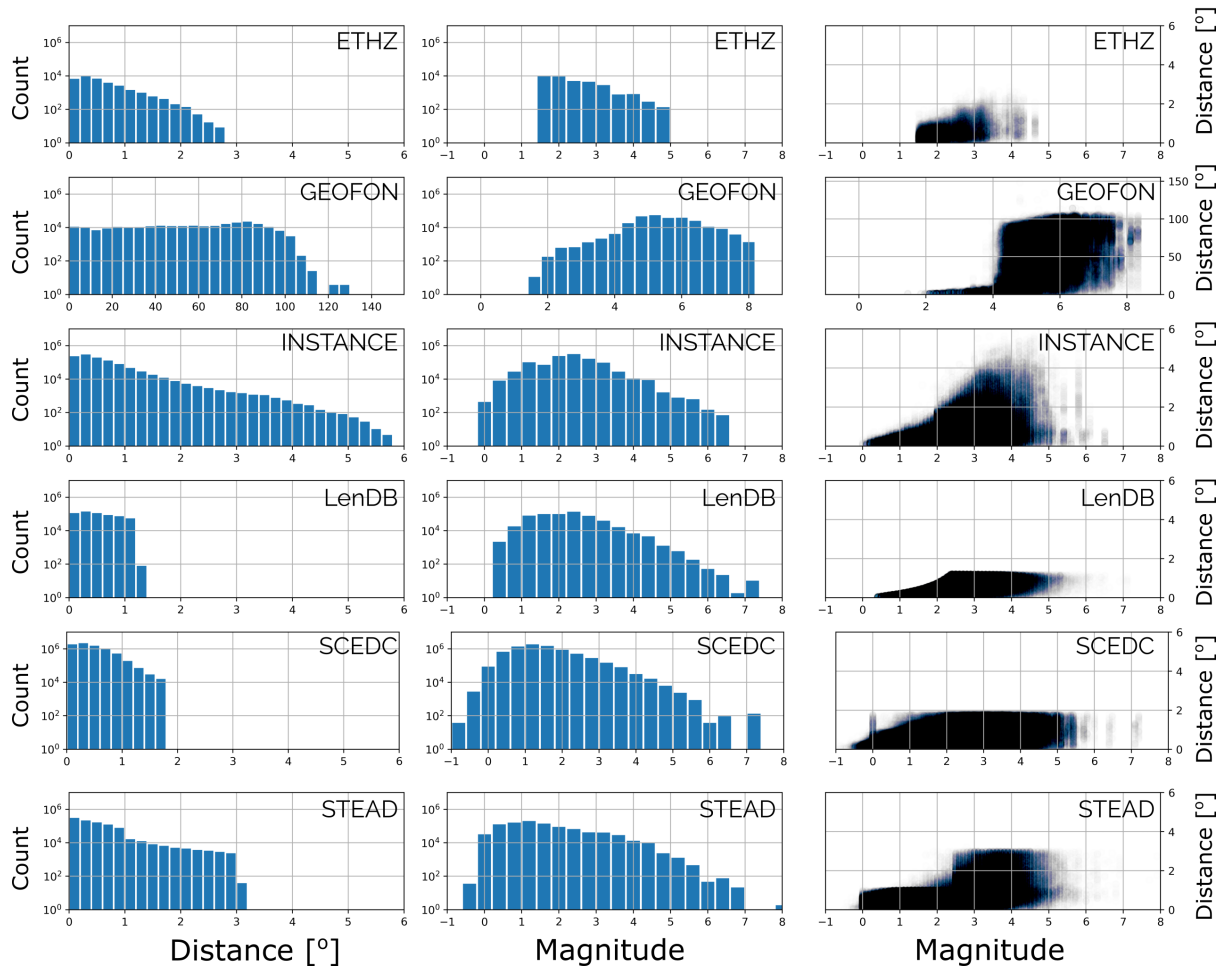


Figure 4: Logarithmic histograms of epicentral distance and magnitude distributions for the datasets with source and station information. For the two-dimensional scatterplot in the last column, all points are plotted with transparency to highlight the overall distribution. The Iquique, NEIC, GPD, Ross2018JGRPick, Ross2018JGRFM, Meier2019JGR datasets are not shown because they are lacking either, magnitude, or source and station location information.

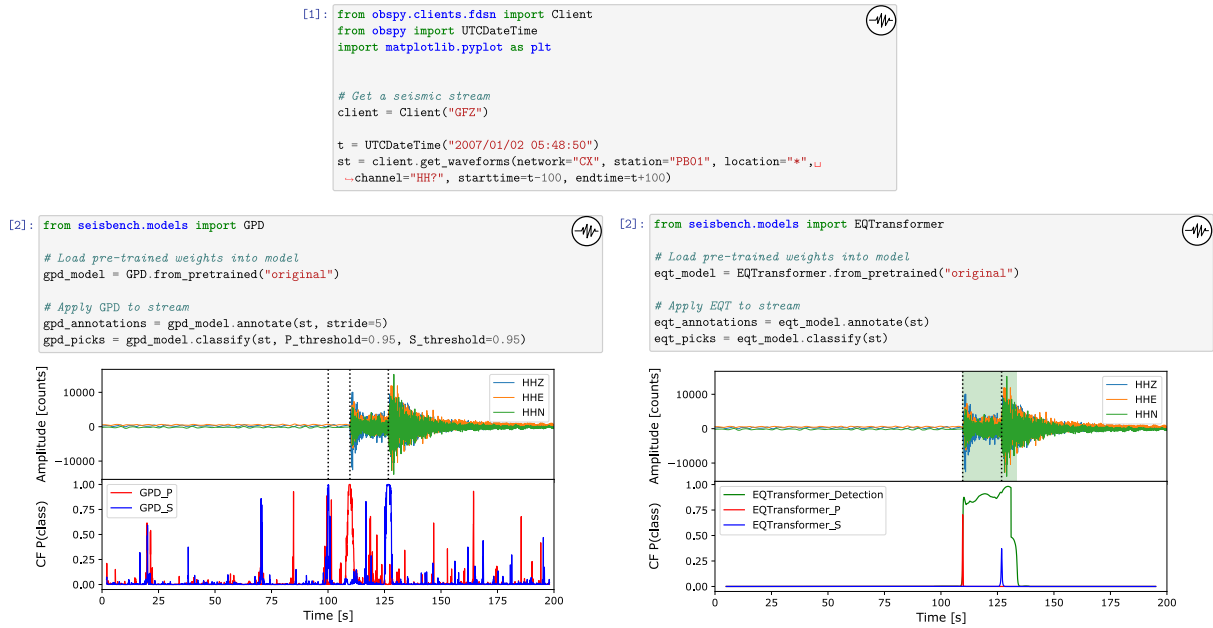
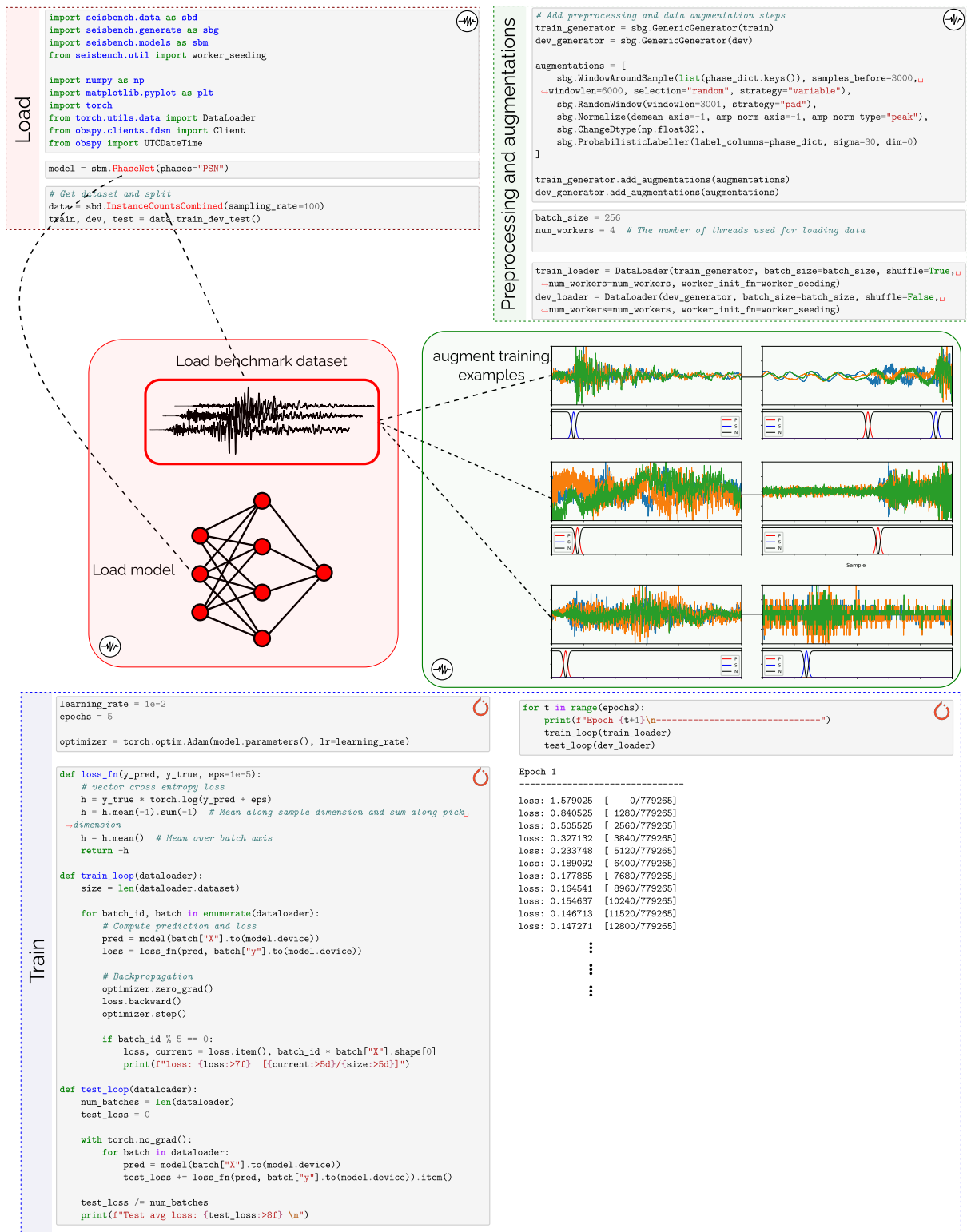


Figure 5: Example code-blocks which download a seismic waveform [1], then loads a pre-trained deep learning picking model and applies the model to predict on the seismic stream using either one of two ML architectures (GPD and EQTransformer) [2]. Resulting picks and characteristic functions from the output probabilities are displayed beneath the code blocks. Characteristic function is abbreviated to "CF". Picks are represented by dotted lines, event detections for the EQT case are the shaded regions. The GPD picker makes a spurious S -pick before the onset of the event but as the original model weights have been incorporated into the pickers to pick on new, unseen data, this example may not be representative of the optimum performance of the respective model architectures, which could be achieved by training on data matched to the application case.



Parameter name	Description
trace_name	A unique identifier for the trace.
trace_start_time	The start time for the trace - if possible following ISO 8601:2004.
trace_sampling_rate_hz	Sampling rate of the trace. If sampling rate is constant across all traces in the data set, it can also be specified in the data_format group in the hdf5 data file.
trace_npts	The number of samples in the trace.
trace_channel	The channel from which the data was obtained without the component identifier, e.g., HH, HN, BH.
trace_category	A category to assign to the trace, e.g. earthquake, noise, mine blast.
trace_snr_db	The signal-to-noise ratio of trace in decibels.
trace_p_arrival_sample	Sample in trace at which P-phase arrives
trace_p_uncertainty_s	Uncertainty of P-phase pick in seconds.
trace_p_weight	The weighting factor assigned to the P-phase pick.
trace_p_status	The status of the P-phase pick, e.g. manual/automatic.
trace_s_arrival_sample	Sample in trace at which S-phase arrives.
trace_s_uncertainty_s	Uncertainty of S-phase pick in seconds.
trace_s_weight	The weighting factor assigned to the S-phase pick.
trace_s_status	The status of the S-phase pick, e.g. manual/automatic.
trace_completeness	The fraction of samples in the trace, which were not filled with placeholder values (between 0 and 1). Placeholder values occur for example in case of recording gaps or missing component traces.
source_id	A unique identifier for the source trace.
source_origin_time	Origin time of the source - if possible following ISO 8601:2004.
source_origin_uncertainty_sec	Uncertainty of source origin time in seconds.
source_latitude_deg	Source latitude coordinate in degrees.
source_latitude_uncertainty_deg	Uncertainty of source latitude coordinate in degrees.
source_longitude_deg	Source longitude coordinate in degrees.
source_longitude_uncertainty_deg	Uncertainty of source longitude coordinate in degrees.
source_depth_km	Source depth in kilometers.
source_depth_uncertainty_km	Uncertainty of source depth coordinate in degrees.
source_error_sec	The error association with the source location in seconds.
source_gap_deg	Azimuthal gap from the source determination in degrees.

source_magnitude	Magnitude value assigned to source.
source_magnitude_type	The type of magnitude calculation used when assigning magnitude to source.
station_network_code	Instrument network code.
station_code	Instrument station code.
station_location_code	Instrument location code.
station_latitude_deg	Instrument latitude in degrees.
station_longitude_deg	Instrument longitude in degrees.
station_elevation_m	Instrument elevation in m.
path_back_azimuth_deg	The backazimuth of phase path from source to receiver in degrees.
path_ep_distance_km	The epicentral distance of source receiver path in kilometers.
path_hyp_distance_km	The hypocentral distance of source receiver path in kilometers.
path_p_travel_s	Travel-time for P-phase in seconds.
path_p_residual_s	Residual of P-phase against some prediction in seconds.
path_s_travel_s	Travel-time for S-phase in seconds.
path_s_residual_s	Residual of S-phase against some prediction in seconds.

Table A1: Example of the parameter naming schema for SeisBench, where metadata parameters follow the naming format guidelines ‘CATEGORY_PARAMETER_UNIT’. The table displays a subset of some of the more common naming parameters. When extending or including new datasets, this can be extended for individual use cases to include any new metadata parameter, providing it adheres to the naming schema.